

Thermochemistry and Dissociation Dynamics of State-Selected C_4H_4X Ions. 3. $C_4H_5N^+$

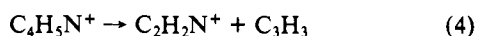
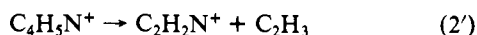
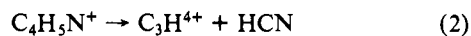
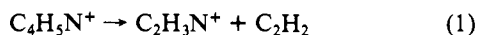
Gary D. Willett¹ and Tomas Baer*

Contribution from the Department of Chemistry, The University of North Carolina at Chapel Hill, Chapel Hill, North Carolina 27514. Received January 31, 1980

Abstract: The photoion-photoelectron coincidence technique has been used to investigate the unimolecular decomposition of the following $C_4H_5N^+$ isomers: pyrrole(1+), methacrylonitrile(1+), allyl cyanide(1+), and cyclopropyl cyanide(1+). Threshold photoelectron spectra and fragment ion photoionization efficiency curves and ion time-of-flight distributions are presented. From a comparison of the measured and statistically calculated absolute unimolecular dissociation rates, it is proposed that following ionization all of the above isomers undergo isomerization to a common precursor which is most likely pyrrole(1+). The associated thermochemistry of the $C_4H_5N^+$ isomers and their respective fragments are discussed in detail. Gaussian-70 4-31G ab initio MO calculations have been used to calculate the relative stabilities of various $C_4H_5N^+$ and $C_2H_3N^+$ structures.

I. Introduction

Dynamical studies on the dissociation of the $C_4H_5N^+$ isomers have been limited to a few mass spectrometric investigations of pyrrole. In 1964, Budzikiewicz et al.^{2a} and Jennings and Boggs^{2b} reported high-mass resolution 70-eV electron impact (EI) mass spectra of pyrrole. Their studies revealed four principal fragmentation pathways in eq 1-4. Except for $C_2H_2N^+$, the intensities



of these ions were within 30% of each other. The intensity of $C_2H_2N^+$, whose nominal mass of 40 is the same as that of $C_3H_4^+$, was a factor of 5 lower. Pyrrole has also been investigated by field ionization³ and photoionization.⁴ In the latter study, only the total ion spectrum was obtained.

In 1971, Derrick and co-workers⁵ investigated the charge-exchange mass spectrum of pyrrole in which primary ions of several recombination energies were used. In their experiment, charge transfer between a simple ion and the pyrrole molecule results in the production of state selected pyrrole(1+). One aim of their study was to correlate dissociation onsets with orbital composition as a guide to the assignment of the molecular electronic structure of pyrrole. In the charge-transfer experiment, ions are prepared with relatively narrow and well-determined internal energies, and so the charge-transfer mass spectra as a function of the ionizing energy constitutes a breakdown diagram. Insight into the reaction dynamics of molecular ions can sometimes be gained by comparing the measured breakdown graph to one calculated with the statistical theory of unimolecular decay. However, Derrick et al.⁵ did not carry out such calculations.

Previous photoion-photoelectron coincidence (PIPECO) studies of the dissociations of various isomeric systems ($C_4H_6^+$,⁶ $C_4H_8^+$,⁷

$C_6H_6^+$,⁸ and $C_8H_8^+$ ⁹) with small reverse activation energies have demonstrated that molecular ion isomerization reactions yielding parent ions in their lowest energy configuration are often faster than dissociation reactions. This is deduced from the fact that the rates of dissociation at equal energies above the fragmentation onset are equal regardless of the structure of the isomer initially ionized. 3-Butyn-2-one, an isomer of furan, represents the first example in the present series of PIPECO studies where the direct dissociation appears to be faster than molecular ion isomerization.¹⁰

The measurement of absolute fragmentation rates using the PIPECO experiment has proven to be a powerful technique for establishing reaction mechanisms and information about the reaction path over the potential energy surface near the onsets of the first few fragmentations. It also provides the most direct experimental evidence with which the statistical theories of mass spectrometry can be tested.

This PIPECO study on the $C_4H_5N^+$ isomers pyrrole, methacrylonitrile, cyclopropyl cyanide, and allyl cyanide represents part of this continuing series of studies on the dissociation dynamics of metastable ions. Here we report the absolute fragmentation rates, threshold photoelectron spectra (TPES), photoionization efficiency (PIE) curves, and fragment ion heats of formation. The experimental procedure has been described in paper 1 of this series.¹¹ The $C_4H_5N^+$ samples were purchased from Aldrich and contained no detectable impurities as determined by photoionization mass spectrometry and TPES.

II. Results

(A) Threshold Photoelectron Spectra. Previous experimental and theoretical studies on the C_4H_5N isomers have concentrated on establishing the electronic structure of pyrrole.^{12,13} He I PES have been reported for cyclopropyl cyanide and allyl cyanide, but we are unaware of any reported spectra for methacrylonitrile.

(1) Pyrrole. The pyrrole TPES over the 8-14-eV photon energy range is shown in Figure 1. Previous studies have established that there are five electronic ion states, $1a_2$ (π , 8.21 eV), $2b_1$ (π , 9.2 eV), $6a_1$ (σ , 12.6 eV), $4b_1$ (σ , 13.0 eV), and $1b_1$ (π , 13.7 eV), that are accessible to 8-14-eV radiation.^{12,13}

A comparison of Figure 1 with the He I PES^{12,13} reveals the same overall spectral features and ionization energies. As in the TPES of other molecules,¹⁴ there is electron signal present in the

(1) Commonwealth Scientific Industrial Research Organization, Post-doctoral Research Fellow, 1978.

(2) (a) H. Budzikiewicz, C. Djerassi, and D. H. Williams, "Mass Spectrometry of Organic Compounds", Holden-Day, San Francisco, 1967, p 596. (b) A. L. Jennings and J. E. Boggs, *J. Org. Chem.*, **29**, 2065 (1964).

(3) I. V. Gol'denfeld, I. Z. Korostyovskii, and V. A. Nazarenko, *Teor. Eksp. Khim.*, **6**, 548 (1970).

(4) V. K. Potapov and B. A. Bazhenov, *High Energy Chem. (Engl. Transl.)*, **4**, 505 (1970).

(5) P. J. Derrick, L. Asbrink, O. Edqvist, B.-O. Jonsson, and E. Lindholm, *Int. J. Mass Spectrom. Ion Phys.*, **6**, 191 (1971).

(6) A. S. Werner and T. Baer, *J. Chem. Phys.*, **62**, 2900 (1975).

(7) T. Baer, D. Smith, B. P. Tsai, and A. S. Werner, *Adv. Mass Spectrom.*, **7A**, 56 (1978).

(8) T. Baer, G. D. Willett, D. Smith, and J. S. Phillips, *J. Chem. Phys.*, **70**, 4076 (1979).

(9) D. Smith, T. Baer, G. D. Willett, and R. C. Ormerod, *Int. J. Mass Spectrom. Ion Phys.*, **30**, 155 (1979).

(10) G. D. Willett and T. Baer, *J. Am. Chem. Soc.*, preceding paper in this issue, No. 2.

(11) J. J. Butler and T. Baer, *J. Am. Chem. Soc.*, preceding paper in this issue, No. 1.

(12) M. von Niessen, L. S. Cederbaum, and G. H. F. Diercksen, *J. Am. Chem. Soc.*, **98**, 2066 (1976), and references cited therein.

(13) L. Asbrink, C. Fridh, and E. Lindholm, *J. Electron Spectrosc. Relat. Phenom.*, **16**, 65 (1979), and references cited therein.

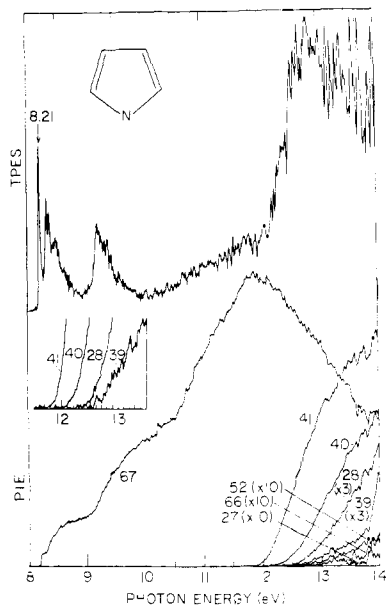


Figure 1. Threshold photoelectron spectrum (TPES) of pyrrole and photoionization efficiency (PIE) curves for $C_4H_5N^+$ (m/e 67), $C_4H_4N^+$ (m/e 66), $C_3H_2N^+$ (m/e 52), $C_2H_3N^+$ (m/e 41), $C_3H_4^+$ (m/e 40), $C_3H_3^+$ (m/e 39), CH_2N^+ (m/e 28), and C_2H_3 (m/e 27).

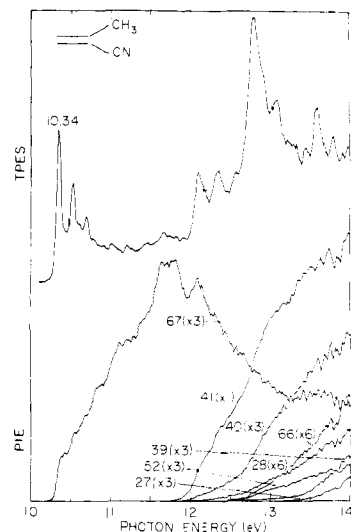


Figure 2. TPES and PIE curves for methacrylonitrile and its fragments.

Franck-Condon gap regions of the first few bands of the TPES. This structure is associated with resonant autoionization which forms ions in highly excited vibrational states.^{8,10,11,14} Derrick et al.⁵ have assigned several Rydberg series converging to the first two electronic ion states of pyrrole. However, the increased electron intensity between 10 and 12 eV in its TPES is a result of autoionization from various Rydberg series which converge to the higher energy ion states. Rydberg transitions such as these are important in the PIPECO experiment since they provide a pathway for the formation of ions of nearly every energy.

(2) Methacrylonitrile. The TPES of methacrylonitrile over the 10–14-eV photon energy range is shown in Figure 2. A comparison of this spectrum with the He I PES of methyl cyanide and allyl cyanide reported by Lake and Thompson¹⁵ readily reveals that the first PE band (vertical and adiabatic IE = 10.34 eV) is associated with the $C=C$ π electrons and that the two small bands at 12.1 and 12.3 eV as well as the larger band at 12.8 eV are associated with the $C\equiv N$ π electrons. The addition of a CH_3

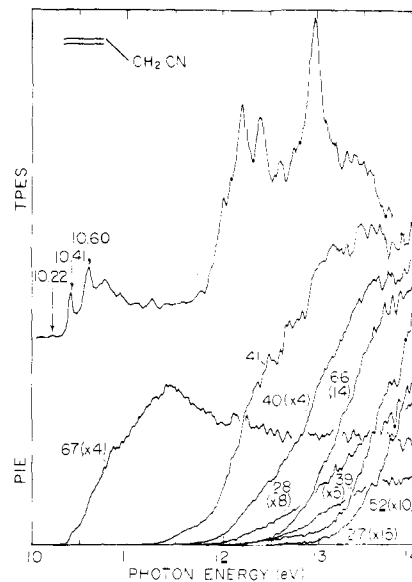


Figure 3. TPES and PIE curves for allyl cyanide and its fragments.

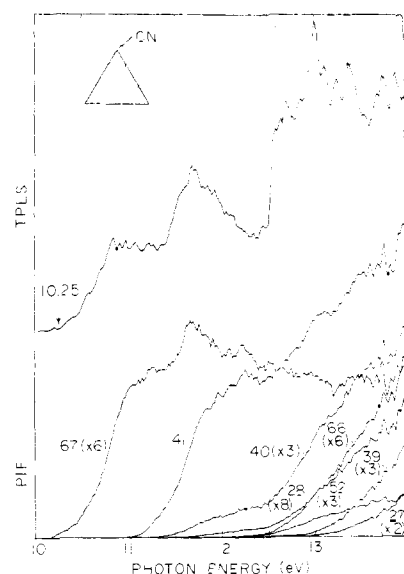


Figure 4. TPES and PIE curves for cyclopropyl cyanide and its fragments.

group to acrylonitrile is expected to produce additional bands around 12 and 14 eV. As in the case of pyrrole, the electron structure in the 11–12-eV photon energy range corresponds to resonant autoionization transitions.

(3) Allyl Cyanide. A comparison of the TPES of allyl cyanide in Figure 3 and the He I PES reported by Lake and Thompson¹⁵ reveals the same overall spectral features. One striking difference is in the intensity of the adiabatic component of the first band. This vibrational component at 10.18 eV can barely be distinguished in the TPES whereas it is quite strong in the He I PES. Vibrational intensity variations such as this are not common place in such comparisons,¹⁴ and in this case, it may arise in the TPES as a consequence of resonant autoionization enhancing the $v = 2, 3$, etc. components. The $v = 0$ peak in the TPES is definitely too intense to be assigned as a hot band.

(4) Cyclopropyl Cyanide. The TPES of cyclopropyl cyanide over the 10–14-eV range is shown in Figure 4. This spectrum reveals the same overall spectral features and ionization energies as those observed with a He I PES reported by Turner and co-workers.¹⁶ The broad nature of the first two Jahn-Teller split

(14) P. T. Murray and T. Baer, *Int. J. Mass Spectrom. Ion Phys.*, **30**, 165 (1979).

(15) R. F. Lake and H. T. Thompson, *Proc. R. Soc. London, Ser. A*, **317**, 187 (1970).

(16) D. W. Turner, C. Baker, A. D. Baker, and C. R. Brundle in "Molecular Photoelectron Spectroscopy", Wiley-Interscience, New York, 1970.

Table I. Thermochemical Data of Neutral Species Relevant to the Dissociation of the Ions $C_4H_5N^+$ (in kcal mol⁻¹)

compd	ΔH_f° 298K ^a
pyrrole	21.2 (l), ^b 15.08 (l), ^c <u>25.88</u> (g) ^c
methacrylonitrile	27.3 (l), ^b <u>31.1</u> (g) ^d
allyl cyanide	28.4 (l), ^b <u>36.9</u> (g) ^d
cyclopropyl cyanide	35.0 (l), ^b <u>45.2</u> (g) ^d
C_2H_2N	51.1 (g), ^e <u>59</u> (g) ^f
C_3H_3	80.7 (g) ^e
CH_2N	<61.0 (g) ^d
HCN	31.2 (g), ^b <u>32.3</u> (g) ^e
C_2H_2	54.2 (g), ^b <u>54.3</u> (g) ^c
CH_3	34.0 (g), ^e <u>34.3</u> (g) ^f
H	52.1 (g) ^e

^a l and g in parentheses refer to the liquid and gas states, respectively. The underlined values are those used in this paper. ^b Reference 17. ^c Reference 18. ^d This work. ^e Reference 19. ^f Reference 20.

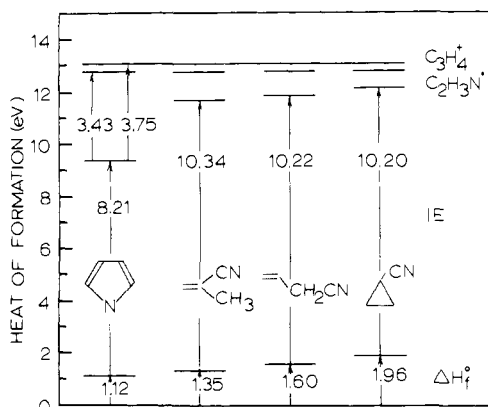
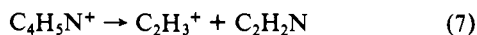
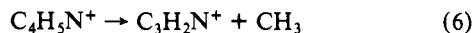
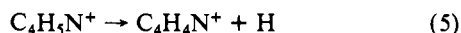


Figure 5. Thermochemistry of the four $C_4H_6N^+$ isomers pyrrole, methacrylonitrile, allyl cyanide, and cyclopropyl cyanide plotted on a heat of formation scale. The heats of formation for the latter three isomers have been determined in this study. The activation energies of 3.43 and 3.75 eV are 0 K values while the other energies are referenced at 298 K.

PE bands centered at 10.9 and 11.7 eV disguises the presence of the resonant autoionization structure which careful band analysis reveals is present in this case also.

(B) Photoionization Efficiency Curves. PIE curves for the $C_4H_5N^+$ molecular ions and associated fragments are illustrated in Figures 1–4. In addition to reactions 1–4, reactions 5–7 were also observed by us over the 8–14-eV photon energy range. Tables I and II and Figure 5 summarize the thermochemical data determined for each of the respective neutral and ionic species described in reactions 1–7.



A complication arises in low-mass resolution studies of the $C_4H_5N^+$ fragmentation since there is the possibility of confusing hydrocarbon fragments with their isobaric fragments containing nitrogen. For example, Kiser and Hobruck²¹ assigned the mass 41 fragment in the dissociation of cyclopropyl cyanide to $C_3H_5^+$, whereas the present results and other high-resolution mass

spectrometric studies on pyrrole^{2a} indicate that it is the $C_2H_3N^+$ fragment.

The measurement of accurate appearance energies (AE) in electron impact and photoionization mass spectrometry, for a variety of reasons, has long posed a problem. Although numerous procedures have been devised for the determination of accurate onsets,^{22–24} we have used a simple linear extrapolation technique. The insert in Figure 1 illustrates some typical ion curve onsets. Such estimates are least accurate when the onsets occur in Franck–Condon gap regions and/or when there is the possibility of collision induced fragmentation processes. Aside from these, the AE's provide us only with upper limits to the thermodynamic dissociation energies because of other factors such as reverse activation energy and kinetic shift.

Kinetic shift raises the AE above the thermodynamic dissociation onset for the first fragment when decay rates at threshold are too slow to allow a sufficient number of ions to fragment during the few microseconds collection time. In the present work, the kinetic shift for mass 41 is estimated to be 0.1 eV and is determined by comparing the measured dissociation rates with the RRKM-calculated rates.

The kinetic shifts for the higher energy fragments arise from competition between the various fragmentation channels. The magnitudes of such shifts are difficult to determine because the mechanism for dissociation at higher energies is usually unknown. For masses 40 and 28, however, since their thermodynamic onsets are known and these fragments appear in regions of high ionization probability, we determine their kinetic shifts to be 0.1 and 0.8 eV, respectively. Because of the numerous above mentioned uncertainties, we have not corrected our onsets for thermal energies, and some of the selected ΔH_f° values in Table II are expressed only as upper limits.

(1) $C_4H_5N^+$. Above the first fragmentation onset, the parent ion yield curves are expected to be flat if direct ionization dominates the ion formation processes. Over the 11–13-eV IE range for pyrrole and methacrylonitrile and to a lesser extent for allyl and cyclopropyl cyanides, there is a peak in the ion yield curves. It is noteworthy that for the former two isomers these maxima correspond to maxima in the autoionization bands in the TPES. This suggests that the same resonant autoionization mechanism is responsible for the increased ion yield in the $C_4H_5N^+$ curve.

(2) $C_4H_4N^+$. Mass 66 is the fourth most intense fragment ion over the 8–14-eV photon energy range for each of the $C_4H_5N^+$ isomers. From the data given in Tables I and II, the ΔH_f° 298K of $C_4H_4N^+$ is $<270 \pm 2$ kcal mol⁻¹. The present AE is almost 1 eV lower than that previously reported by Derrick et al.⁵

(3) $C_3H_2N^+/C_4H_4^+$. For the remainder of the fragmentation reactions, the possibility of formation of the hydrocarbon and/or N-containing fragments needs to be considered. The lowest energy $C_4H_4^+$ ion has probably a cyclic structure with a ΔH_f° of 278 ± 2 kcal mol⁻¹.⁸ Combining this with the ΔH_f° (NH) of 79 kcal mol⁻¹¹⁹ yields a calculated onset for mass 52 from pyrrole of 14.35 eV which is nearly 2 eV above the measured onset of 2.50 eV. Therefore, mass 52 must be the $C_3H_2N^+$ fragment.

(4) $C_2H_3N^+/C_3H_5^+$. For each of the $C_4H_5N^+$ isomers, mass 41 is the most abundant fragment over the 8–14-eV photon energy range. Kiser and Hobruck in 1962 proposed that mass 41 produced in the dissociation of cyclopropyl cyanide was cyclic $C_3H_5^+$.²¹

There are two reasons for doubting this assignment. First, a high-mass resolution study^{2a} of pyrrole at low ionizing energies indicated that mass 41 is due entirely to $C_2H_3N^+$. Because our lifetime studies show that at low energies cyclopropyl cyanide isomerizes to pyrrole prior to dissociation, the two parent ions must produce the same fragment. Second, the heat of formation of the $C_3H_5^+$ fragment, based on our AE and a ΔH_f° of CN of 104 kcal mol⁻¹,¹⁹ would be 195 kcal mol⁻¹, significantly lower than the 225 kcal mol⁻¹¹⁹ for the linear fragment. Because the cyclic isomer

(17) D. R. Stull, E. F. Westrum, and G. C. Sinke in "The Chemical Thermodynamics of Organic Compounds", Wiley, New York, 1969.

(18) J. D. Cox and G. Pilcher in "Thermochemistry of Organic and Organometallic Compounds", Academic Press, New York, 1970.

(19) H. M. Rosenstock, K. Draxl, B. W. Steiner, and J. T. Herron in "Energetics of Gaseous Ions", *J. Phys. Chem. Ref. Data*, **6**, (1) (1977).

(20) S. W. Benson in "Thermochemical Kinetics", Wiley, New York, 1976.

(21) R. W. Kiser and B. G. Hobruck, *J. Phys. Chem.*, **66**, 957 (1962).

(22) J. H. Beynon, R. G. Cooks, K. R. Jennings, and A. J. Ferrer-Correia, *Int. J. Mass Spectrom. Ion Phys.*, **18**, 87 (1979).

(23) A. S. Werner, B. P. Tsai, and T. Baer, *J. Chem. Phys.*, **60**, 3650 (1974).

(24) W. A. Chupka, *J. Chem. Phys.*, **54**, 1936 (1971).

Table II. Appearance Energies and (ΔH_f°) of Ionic Fragments^a

	$C_4H_4N^+$	$C_3H_2N^+$	$C_2H_3N^+$	$C_3H_4^+$	$C_3H_3^+$	CH_2N^+	$C_2H_3^+$
pyrrole, $c-C_4H_5N$	12.85 (270.1)	12.50 (279.8)	11.75 (242.5)	12.00 (270.3)	12.60 <i>b</i>	12.40 (231.1)	13.60 (280.0)
methacrylonitrile, $CH_2C(CH_3)CN$	12.55 (268.4)	12.20 (278.1)	11.65 (245.5)	11.75 (269.8)	12.30 <i>b</i>	12.05 (228.3)	13.20 (276.5)
allyl cyanide, CH_2CHCH_2CN	12.30 (268.5)	12.05 (280.5)	11.10 (238.6)	11.50 (269.8)	12.10 <i>b</i>	11.90 (230.6)	12.90 (275.4)
cyclopropyl cyanide, $c-C_3H_3CN$	12.10 (272.1)	11.75 (281.9)	11.00 (244.6)	11.20 (271.2)	(11.80) <i>b</i>	11.50 (229.7)	12.65 (277.9)
selected ΔH_f° _{298K}	<269.7 ± 1.8	<280.3 ± 1.5	240.0 ± 1.0 ^c	269.2 ^d	256 ^d	<230.1 ± 1.0	269.2 ^d

^a Appearance energies and ΔH_f° in eV and kcal mol⁻¹, respectively. ^b Used known $\Delta H_f^\circ(C_3H_3^+)$ to determine $\Delta H_f^\circ(CH_2N)$ in Table II. ^c Based on RRKM fit of decay rates. Values taken from ref 19.

is not stabilized by aromaticity (as is for instance $C_3H_3^+$), there is no reason for expecting the cyclic isomer of $C_3H_5^+$ to be 30 kcal mol⁻¹ more stable than the linear one. Therefore at energies below 14 eV, mass 41 is certainly the $C_2H_3N^+$ ion. Its ΔH_f° is calculated to be 240.0 ± 1.0 kcal mol⁻¹. This value is based on the RRKM theory analysis of the ion lifetimes (see section C).

The most obvious structure for $C_2H_3N^+$ is methyl cyanide or methyl isocyanide; however, a thermochemical analysis readily reveals that these isomers would have fragmentation onsets that are ~2 eV higher than those measured and so a lower energy isomer must exist. This is discussed in more detail in section IIIB.

(5) $C_2H_2N^+/C_3H_4^+$. Budzikiewicz et al.^{2a} have previously shown that the mass 40 peak for pyrrole is comprised of the $C_3H_4^+$ and $C_2H_2N^+$ fragments in a 4.5:1 intensity ratio, respectively. They proposed that expulsion of the stable HCN neutral fragment is the driving force for the larger production of the $C_3H_4^+$ ion. Derrick et al.,⁵ however, have assigned the mass 40 peak in their charge-transfer mass spectrum to a $C_2H_2N^+$ structure.

To identify the m/e 40 peak at low energies, we carried out a high-mass resolution, low ionizing energy study on pyrrole.²⁵ Our results show that the $C_2H_2N^+$ fragment does not onset with significant intensity until an electron-impact energy of about 17 eV.

Since all of the measured heats of formation for this fragment listed in Table II are only 1–2 kcal mol⁻¹ above the known ΔH_f° of allene(1+) ($\Delta H_f^\circ = 269.2$ kcal mol⁻¹), we can be certain that this fragment is allene(1+).

(6) $C_2HN^+/C_3H_3^+$. Mass 39 is the most intense fragment in the 70-eV electron-impact high-mass resolution spectrum of pyrrole^{2a} and consists of 99% C_3H_3 . Each of the mass 39 ion yield curves shown in Figures 1–4 show an increase in intensity about 1 eV above their onsets which can be attributed to the formation of the propargyl ion isomer. Presumably below this energy, the cyclopropenium ion is formed.

If we use a $C_3H_3^+$ ΔH_f° of 256 kcal mol⁻¹⁸ and the AE's listed in Table II, we can estimate that the ΔH_f° _{298K} for CH_2N is <61 kcal mol⁻¹.

(7) $CH_2N^+/C_2H_4^+$. The high-mass resolution spectrum of pyrrole^{2a} indicates that mass 28 is entirely CH_2N^+ . If we were to assume the opposite, that at low energies mass 28 was $C_2H_4^+$, we would calculate a ΔH_f° of C_2HN of 55 kcal mol⁻¹. Since the ΔH_f of C_2H_3N and C_2H_2N are known to be 21 and 51 kcal mol⁻¹, respectively,¹⁹ it seems unlikely that C_2HN would have a ΔH_f° of 55 kcal mol⁻¹.

We previously determined the ΔH_f° of CH_2N to be <61 kcal mol⁻¹, and since we have measured the ΔH_f° of CH_2N^+ (see Table II) to be <230 kcal mol⁻¹, the adiabatic ionization energy of the fragment CH_2N should be approximately 7.3 eV.

(8) $CNH^+/C_2H_3^+$. Mass 27 has the lowest ion yield for each of the $C_4H_5N^+$ isomers, and as a result of low photon intensity and high AE, it can barely be observed in the PIE curve of pyrrole.

A thermochemical analysis reveals that this fragment cannot be HCN^+ since all of the mass 27 AE's listed in Table II are ~2

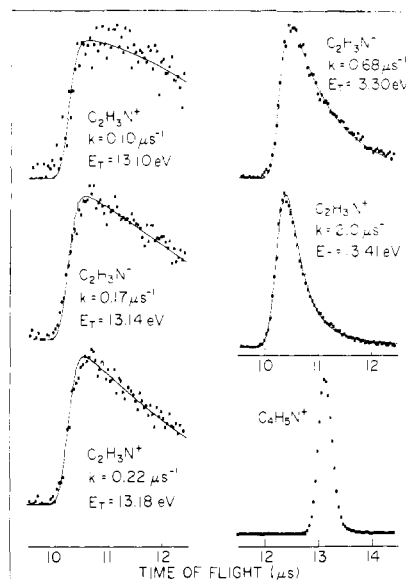


Figure 6. Representative coincidence time-of-flight distribution for the $C_2H_3N^+$ fragment produced from state-selected pyrrole, $C_4H_5N^+$, at total internal energies, E_T . (E_T = photon energy plus ΔH_f° of pyrrole.) The solid lines represent the calculated time-of-flight distributions determined by using the indicated fragmentation rates, k .

eV below its thermodynamic onset. This ion then is most likely $C_2H_3^+$.

(C) Unimolecular Decay Rates. Figure 6 illustrates typical coincidence time-of-flight (TOF) distributions for the $C_2H_3N^+$ fragment at several internal energies, E_T . E_T is equal to the sum of the photon energy and the ΔH_f° of the C_4H_5N isomer. Only the spectra recorded for pyrrole are reproduced here since the TOF distributions, recorded both with and without the quadrupole mass filter for the other $C_4H_5N^+$ isomers, were similar. Counting times ranged between 5 and 35 h.

The solid lines shown in Figure 6 represent the calculated TOF distributions determined by using the indicated fragmentation rates. These calculated TOF distributions are fitted to the experimental data by using the ion acceleration field and parent and fragment ion masses. There are only two adjustable parameters in the calculation, the mean ion lifetime and kinetic energy (KE) released on dissociation. KE release and the TOF broadening resulting from the quadrupole mass filter are accounted for by convoluting the calculated TOF distribution with the parent ion TOF distribution shown in Figure 6. This approach is considerably faster than, but indistinguishable from, the more exact method of summing over a distribution of KE releases and ion lifetimes especially for cases such as the $C_4H_5N^+$ isomers where the KE releases are small.

A small correction which affects the derived rate by less than 50% is required to account for the contamination of the ion energy selection by hot electrons which pass through the collimated hole structure. Near the dissociation onset, the measured rates for cyclopropyl cyanide are higher than might be expected most likely

(25) These experiments were carried out at the Research Triangle Park Mass Spectrometry Facility on an MS 902 instrument.

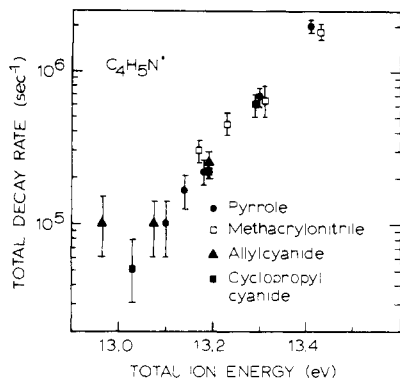


Figure 7. Unimolecular decay rates for the state selected $C_4H_5N^+$ isomers as a function of their respective total internal energies (= photon energy plus heat of formation of $C_4H_5N^+$).

because the data have not been corrected for contributions from scattered light. This contribution is most pronounced there because of the long collection times.

Experimental fragmentation rates for the production of $C_2H_3N^+$ for each of the $C_4H_5N^+$ isomers are plotted as a function of E_T in Figure 7. To within about 0.06 eV in E_T , the rates measured for the cyclopropyl and allyl cyanides are equal to those of pyrrole. For methacrylonitrile however, the rates were shifted to higher energy by 0.16 eV. Because of the uncertainty in the heats of formation of these last three isomers, we assume that the rates, in fact, are identical with those of pyrrole and accordingly have adjusted their ΔH_f° . This leads to heats of formation of 31, 37, and 45 kcal mol⁻¹ for methacrylonitrile, allyl cyanide, and cyclopropyl cyanide, respectively.

The onset for the $C_3H_4^+$ fragment also falls in the metastable energy range and so we are able to compare the rates of production of $C_2H_3N^+$ and $C_3H_4^+$. The fact that these two rates are identical at the same values of E_T confirms that reactions 1 and 2 are in competition over this energy range. By utilizing the following PIPECO branching ratios for $C_3H_4^+ : C_2H_3N^+$ of 1:32, 1:17, and 1:9 at total internal energies of 13.18, 13.30, and 13.41 eV, respectively, together with the total rates of disappearance of $C_4H_5N^+$ listed in Figure 7, we can determine the absolute rates of production of $C_2H_3N^+$ and $C_3H_4^+$ by using a similar method to that previously described for furan(1+).¹⁰ These rates are plotted as a function of E_T in Figure 8.

III. Discussion

(A) $C_4H_5N^+$ Isomerization. According to the statistical theory, the rate of fragmentation is inversely proportional to the parent ion density of states, $\rho(E)$.²⁶ Since $\rho(E)$ increases sharply with energy and the four $C_4H_5N^+$ isomers have different activation energies for the production of $C_2H_3N^+$ (Figure 5), they are expected to have substantially different fragmentation rates. Our RRKM calculations predict a difference of 10^4 between the extreme cases of pyrrole and cyclopropyl cyanide at $E_T = 13$ eV.

As with other isomeric systems investigated by the PIPECO technique,⁶⁻⁹ the fact that all the isomers have identical rates for reaction 1 over the metastable energy range indicates that the excited $C_4H_5N^+$ ions sample a common-phase space which is independent of the initial precursor ion. In other words, all four isomers rearrange to a common precursor prior to fragmentation.

It must be stated however that this conclusion is valid only in the metastable energy range and that at higher energies the fragmentation rates may well become competitive with those of isomerization.⁸

It seems probable that the three higher energy isomers rearrange to the lowest energy isomer which is most likely pyrrole. Holmes and Terlouw²⁷ have shown that vinyl ketene is a $C_4H_4O^+$ isomer that is as least as stable as furan(1+) and it is possible that a

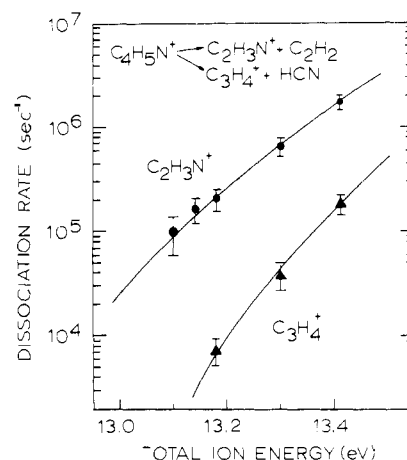


Figure 8. Dissociation rates of $C_4H_5N^+$ to the two product channels, $C_2H_3N^+$ and $C_3H_4^+$. The points represent the experimental rates determined from the total dissociation rates (Figure 7) and the PIPECO branching ratios (section IIC). The solid lines are the RRKM calculated rates by assuming a pyrrole molecular ion, the loose transition-state frequencies of Table III, and the energies in Figure 5.

similar isomer exists for the $C_4H_5N^+$ isomers. Our MO calculations described in the next section however indicate that the isoelectronic isomer vinyl ketenimine(1+) is considerably less stable than pyrrole(1+).

(B) Molecular Orbital Calculations. We have used the Gaussian-70 ab initio LCAO-SCF molecular orbital program at the 4-31G basis set level.²⁸ The geometries were optimized with this basis set and the relative energies of several $C_4H_5N^+$ and $C_2H_3N^+$ isomers were compared. Despite the neglect of correlation energy²⁹ and the relatively restricted 4-31G basis set, our results are in semiquantitative agreement with experimental energies where comparisons can be made. We did not have access to the more accurate 6-31G* basis set where inclusion of d orbitals is known to improve the calculated energies, especially for cyclic, ionic systems.^{29,30}

(1) $C_4H_5N^+$. Vinyl ketene(1+) has been shown experimentally to be as stable as furan(1+). Pyrrole is isoelectronic with furan. It is therefore of interest to determine the relative energies of the isomers, vinyl ketenimine(1+) and pyrrole(1+). We are unaware of any thermochemical information pertaining to vinyl ketenimine so that the ab initio calculations are our only "data". The total energy of pyrrole(1+) determined by using the ab initio geometry of Tanaka et al.³¹ was -206.0312 au while that for the partially optimized vinyl ketenimine was -205.9580 au. These results indicate that pyrrole(1+) is more stable than vinyl ketenimine(1+) by about 2 eV. This difference is well beyond the accuracy of these calculations. We, thus, conclude that pyrrole(1+) is more stable than vinyl ketenimine(1+).

(2) $C_2H_3N^+$. In a recent study, van Thuijl et al.³² have examined the collision induced dissociation of $C_2H_3N^+$ fragments formed from several different molecules in a mass spectrometer. On the basis of the similarity of these spectra, they proposed that the four isomers examined by us as well as butyronitrile and crotonitrile all produce the same $C_2H_3N^+$ fragment whose structure they assumed to be that of ketenimine(1+). In contrast, the collision-induced dissociation spectra of CH_3CN and CH_3NC were very different. These results agree with our own conclusions which are based on the ΔH_f° of the $C_2H_3N^+$ fragment. In order to confirm these results and possibly to predict a structure for the

(26) W. Forst in "Theory of Unimolecular Reactions", Academic Press, New York, 1973.

(27) J. L. Holmes and J. K. Terlouw, *J. Am. Chem. Soc.*, **101**, 225 (1979).

(28) R. Ditchfield, W. J. Hehre, and J. A. Pople, *J. Chem. Phys.*, **54**, 724 (1971).

(29) J. A. Pople, *Int. J. Mass Spectrom. Ion Phys.*, **19**, 89 (1976).

(30) L. Radom, P. C. Hariharan, J. A. Pople, and P. v. R. Schleyer, *J. Am. Chem. Soc.*, **98**, 10 (1976).

(31) E. Tanaka, T. Nomura, T. Noro, H. Tatewaki, T. Takada, H. Kashiwagi, F. Sasaki, and K. Ohno, *J. Chem. Phys.*, **67**, 5738 (1977).

(32) J. van Thuijl, J. J. van Houte, A. Maquestian, R. Flammang, and C. DeMeyer, *Org. Mass Spectrom.*, **12**, 196 (1977).

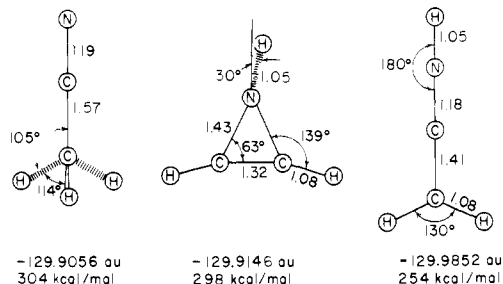


Figure 9. Optimized geometries and energies of three $C_2H_3N^+$ isomers calculated with the Gaussian 70 4-31G molecular orbital program. The ΔH_f° of methyl cyanide is taken from reference 19.

most stable $C_2H_3N^+$ ion, we carried out calculations on $C_2H_3N^+$ structures.

The total energies in atomic units and the heats of formation of optimized geometries for three $C_2H_3N^+$ isomers are shown in Figure 9. All the indicated angles and bond lengths (in angstroms) were optimized. These results show that ketenimine(1+) is indeed more stable than the other two isomers by over 2 eV. The ab initio calculations are not particularly useful for calculating heats of formation, i.e., the energy with respect to the standard states of the naturally occurring elements. However, if one of the isomers has a known heat of formation, the ΔH_f° for the other isomers can be calculated with reasonable accuracy. The ΔH_f° of methyl cyanide(1+) is 304 kcal mol⁻¹.¹⁹ Using this value, we calculate the ΔH_f° of ketenimine(1+) to be 254 kcal mol⁻¹. This is reasonably close to the experimentally measured $C_2H_3N^+$ fragment ΔH_f° of 240 kcal mol⁻¹ (Table II), to suggest that ketenimine(1+) is very likely the most stable structure of $C_2H_3N^+$. Somewhat surprising is that for the most stable structure, the H atom attached to the nitrogen atom was found to lie in the plane of the ion.

It is of some interest to compare the geometry of the methyl cyanide ion with that of the neutral. In the latter, the CC and CN bond lengths are 1.53 and 1.14 Å, respectively, both considerably shorter than in the ion. The longer CN bond in the ion is consistent with the interpretation of the reduced CN stretch frequency in the PES of methyl cyanide.³³

(C) The Comparison with the Statistical Theory. One of the primary purposes of this work is to examine the applicability of the statistical theory²⁶ in describing metastable dissociation mechanisms for a system in which the absolute decay rates are known as a function of total internal energy. To carry out such a comparison using the RRKM theory, it is necessary to know accurate heats of formation of the parent ion and associated fragments together with the vibrational frequencies of the molecular ion and transition state. Such data are rarely available even for the parent molecular ion and so certain assumptions must be made.

Guided by the thermochemical data of Figure 5, we have assumed that the molecular ion structure involved in the dissociation is that of pyrrole. For a stable ion such as pyrrole, the vibrational frequencies of the ion are not expected to vary significantly from those of the molecule; hence, the molecular ion density of states can be calculated with reasonable accuracy by assuming the molecular frequencies.³⁴

The choice of frequencies for the transition state is more difficult because its structure is not amenable to experimental investigation. Nevertheless for dissociation reactions in which there are small reverse activation energies, it is reasonable to propose a transition state geometry that is close to the structure of the final product. This principle is often referred to as the Hammond

Table III. Fundamental Vibrational Frequencies for the Vinyl Ketene Transition State Used in the RRKM Calculations^a (in cm⁻¹)

C-H and N-H stretches	3118, 3102, 3028, 3000, 3408
C-C stretch and torsion	1158, 157
C=C and C=N stretches	1388, 1625, 1645 ^b
CH scissors, rock, wag and twist	1420, 912, 959, 593
C-H and N-H bends	1275, 1275, 993, 993, 1143, 558
CCC, CCN, and CCCC bend, torsion, and deformation	530, 450, 340, 100

^a Normal-mode frequencies are estimated from those of related molecules given in ref 36 and 37. ^b Reaction coordinate.

postulate.³⁵ Since we have already proposed the ketenimine and allene structures for masses 41 and 40, respectively, it is reasonable to choose vinyl ketenimine(1+) as the transition state. It should be stressed, however, that this choice is not particularly critical. Vinyl ketenimine is merely representative of a "loose" transition state compared to, for instance, pyrrole which is a "tight" transition state. We are unaware of any experimentally measured vibrational frequencies for vinyl ketenimine and so those listed in Table III were estimated from those of related molecules.^{36,37}

The final parameters required for the RRKM calculations are the activation energies for the production of $C_2H_3N^+ + C_2H_2$ and $C_3H_4^+ + HCN$. The ΔH_f° of $C_2H_3N^+$ is not known, and we, therefore, used it as an adjustable parameter. The RRKM rates were calculated by using the Hase-Bunker program³⁸ in which a semiclassical Whitten-Rabinovitch state counting option is used. A comparison of the calculated rates of production of $C_2H_3N^+$ and $C_3H_4^+$ and their corresponding experimental rates is shown in Figure 8. There is close agreement between the calculated (solid lines) and experimental (points) rates for both reactions 1 and 2. A ΔH_f° of 240 ± 1 kcal mol⁻¹ for $C_2H_3N^+$ was derived from these calculations. A calculation with a "tight" transition state (pyrrole frequencies) gave rates which were nearly 2 orders of magnitude lower. The thermochemical onset for the $C_2H_3N^+$ fragment could not be adjusted to allow the "tight" transition state to fit the rates for both $C_2H_3N^+$ and $C_3H_4^+$ production because the latter onset is well established.

The pyrrole dissociation is dramatically different from the furan dissociation in which the isomerization via a tight transition state was the rate-determining step.¹⁰

IV. Conclusion

The measurement of identical lifetimes for several $C_4H_5N^+$ isomers indicates that over the total energy range 12.9–13.4 eV all isomers rearrange to a common precursor. The results of statistical theory calculations are consistent with the assumption that this precursor has a pyrrole structure and that the transition state for the dissociation is "loose".

Gaussian 70 4-31G ab initio molecular orbital calculations show that vinyl ketenimine(1+) is less stable than pyrrole(1+). Finally, the linear ketenimine structure for the $C_2H_3N^+$ ion was found to be over 2 eV more stable than either the cyclic ketenimine or methyl cyanide. It is, therefore, a good candidate for the most stable $C_2H_3N^+$ ion. The experimentally measured difference between the ΔH_f° of methyl cyanide and the $C_2H_3N^+$ formed in the dissociation is 2.78 eV.

Acknowledgment. We are grateful to L. G. Pedersen for supplying us with his modified version of the Gaussian 70 4-31G ab initio program and for several helpful discussions. This work was supported by the National Science Foundation.

(33) D. C. Frost, F. G. Herring, C. A. McDowell, and J. A. Stenhouse, *Chem. Phys. Lett.*, **4**, 533 (1970).

(34) R. C. Lord and F. A. Miller, *J. Chem. Phys.*, **10**, 328 (1942).

(35) G. S. Hammond, *J. Am. Chem. Soc.*, **77**, 334 (1955).

(36) M. J. S. Dewar and G. P. Ford, *J. Am. Chem. Soc.*, **99**, 1685 (1977).

(37) T. Shimanouchi, *Natl. Stand. Ref. Data Ser. (U.S., Natl. Bur. Stand.)*, NSRDS-NBS 39 (1972).

(38) Available as program 234 through the Quantum Chemistry Program Exchange, Indiana University.